Characterization of the Ternary Mixture of Sphingomyelin, POPC, and Cholesterol: Support for an Inhomogeneous Lipid Distribution at High Temperatures

Andreas Bunge,* Peter Müller,† Martin Stöckl,† Andreas Herrmann,† and Daniel Huster*‡

*Junior Research Group "Structural Biology of Membrane Proteins", Institute of Biotechnology, Martin-Luther University Halle-Wittenberg, Halle, Germany; †Institute of Biology/Biophysics, Humboldt-University Berlin, Berlin, Germany; and ‡Institute of Medical Physics and Biophysics, University of Leipzig, Leipzig, Germany

ABSTRACT A ternary lipid mixture of palmitoyl-oleoyl-phosphatidylcholine (POPC), palmitoyl-*erythro*-sphingosylphosphorylcholine (PSM), and cholesterol at a mixing ratio of 37.5:37.5:25 mol/mol/mol was characterized using fluorescence microscopy, ^{2}H NMR, and electron paramagnetic resonance spectroscopy. The synthetic PSM provides an excellent molecule for studying the molecular properties of raft phases. It shows a narrow phase transition at a temperature of 311 K and is commercially available with a perdeuterated *sn*-2 chain. Fluorescence microscopy shows that large inhomogeneities in the mixed membranes are observed in the coexistence region of liquid-ordered and liquid-disordered lipid phases. Above 310 K, no optically detectable phase separation was shown. Upon decrease in temperature, a redistribution of the cholesterol into large liquid-ordered PSM/cholesterol domains and depletion of cholesterol from liquid-disordered POPC domains was observed by ^{2}H NMR and electron paramagnetic resonance experiments. However, there is no complete segregation of the cholesterol into the liquid-ordered phase and also POPC-rich domains contain the sterol in the phase coexistence region. We further compared order parameters and packing properties of deuterated PSM or POPC in the raft mixture at 313 K, i.e., in the liquid crystalline phase state. PSM shows significantly larger ^{2}H NMR order parameters in the raft phase than POPC. This can be explained by an inhomogeneous interaction of cholesterol between the lipid species and the mutual influence of the phospholipids on each other. These observations point toward an inhomogeneous distribution of the lipids also in the liquid crystalline phase at 313 K. From the prerequisite that order parameters are identical in a completely homogeneously mixed membrane, we can determine a minimal microdomain size of 45–70 nm in PSM/POPC/cholesterol mixtures above the main phase transition of all lipids.

INTRODUCTION

Ever since the fluid mosaic model of biological membranes was established in 1972 (1), the question has been raised whether the lipid molecules of the bilayer are homogeneously mixed or the membrane represents a well-balanced mixture of small domains and lateral inhomogeneities. More than 30 years ago, model studies in binary phospholipid mixtures have shown that chain-length differences of four methylene groups can already trigger lateral demixing (2,3). When lateral lipid domains, also called rafts, were first found in biological membranes in 1997 (4), it became obvious that lateral segregation of the membrane constituents is not just a physicochemical effect of model membranes but plays significant biological roles in protein sorting, lipid trafficking, protein ligand interaction, or signal transduction across the membrane (5–10). While rafts have been identified in mammalian, plant, and yeast cells and details about their lipid and protein composition are clear, there is still significant uncertainty about the biophysical properties of the lipid molecules in a raft, the size of rafts, and the dynamic reorganization of all molecules in rafts. Although model systems can help our understanding of issues such as raft size, packing properties of the lipid molecules in rafts, or their phase state, it is still a matter of discussion to which degree results from model membranes can reflect the situation in the biological membrane.

Ternary mixtures of sphingomyelin (SM), unsaturated phosphatidylcholines (PC), and cholesterol represent the standard model system for the outer leaflet of eukaryotic cell membranes. For these mixtures, the formation of large lipid domains can be triggered by decreasing the temperature, which is conveniently visualized by fluorescence microscopy (11–14). Further, ^{2}H solid-state nuclear magnetic resonance (NMR) spectroscopy has significantly contributed to our understanding of the molecular properties in these domains (14–17). Essentially, naturally existing sphingomyelins feature saturated acyl chains. In contrast, in most biologically relevant PC species, the *sn*-1 position is saturated and the *sn*-2 chain contains varying degrees of unsaturation in the form of *cis*-double bonds (18).

In this study, the ternary mixture of *N*-palmitoyl-*D*-*erythro*-sphingosylphosphorylcholine (PSM), palmitoyl-oleoyl-phosphatidylcholine (POPC), and cholesterol was studied. Although both phospholipids share the same headgroup, the hydrophobic parts of the molecules are very different (see Fig. 1). The *trans*-double bond between C_4 and C_5 of the sphingosine chain, the amide group, and the free hydroxyl are important

Submitted May 15, 2007, and accepted for publication November 9, 2007.

Address reprint requests to Daniel Huster, Tel.: 49-0-345-552-4942; E-mail: daniel.huster@biochemtech.uni-halle.de.

Editor: Anthony Watts.

0006-3495/08/04/2680/11 $2.00

doi: 10.1529/biophysj.107.112904

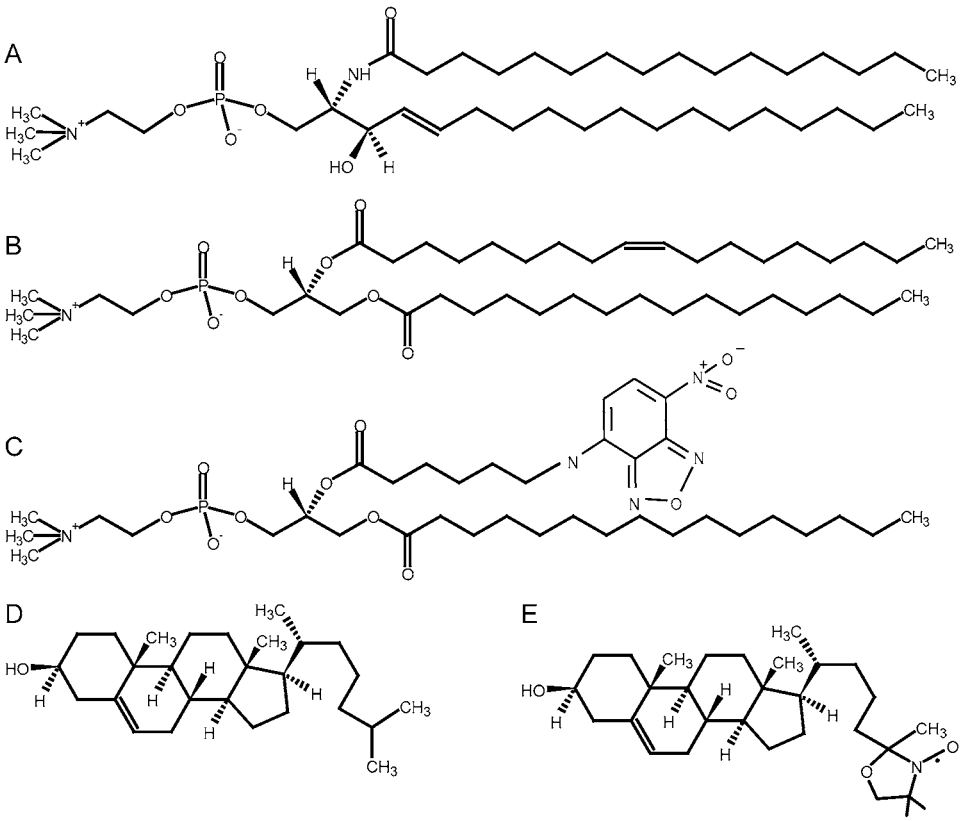

FIGURE 1 Chemical structures of the lipids used in this study: (*A*) PSM, (*B*) POPC, (*C*) NBD-PC, (*D*) cholesterol, and (*E*) 25-doxyl-cholesterol.

features of PSM. POPC exhibits one saturated 16:0 and one unsaturated 18:1 chain with two ester carbonyls. Thus sphingomyelins carry hydrogen-bond acceptor and donor properties, which qualify the molecule for inter- and intramolecular interactions. In contrast, POPC can only act as a hydrogen-bond acceptor (19). As a consequence of the saturated chains, SM shows a tighter packing in the membrane (20). Because of these features, a relative high-melting temperature of the sphingomyelins and a low-melting temperature of unsaturated phosphatidylcholines is observed (21).

In contrast to the phospholipids, cholesterol consists of a rigid ring system and a short branched hydrocarbon chain. It inserts into lipid membranes with its hydroxyl group oriented toward the membrane surface and an orientation of the long axis parallel to the bilayer-normal (22). Cholesterol has important effects on the lateral organization of the phospholipids in the membrane. It increases the molecular order of the acyl chains of phospholipids, which leads to an increase of the bilayer thickness by modulating the packing of the lipids in the membrane (23–25) This effect, called condensation, has been shown to be much stronger for saturated lipids than for their unsaturated counterparts (26,27).

It is known that increasing amounts of cholesterol in model membranes composed of SM as the high-melting lipid and unsaturated PC as the low-melting lipid will induce a lateral separation of a primary homogeneous lipid phase into liquid-ordered (l_o) and liquid-disordered (l_d) domains. The l_o phase state is rich in SM and cholesterol and characterized by a high lateral mobility and rapid axially symmetric rotations of the lipids similar to the lamellar liquid-crystalline state (L_α). But in contrast to the L_α phase, the acyl-chain order is high in the l_o phase state, comparable to the lamellar gel phase L_β (28). The l_d domains exhibit a low cholesterol content; the lipids are loosely packed and diffuse relatively freely. The formation of ordered domains is probably caused by the favorable van der Waals interactions of the rigid ring system of cholesterol with the saturated chains of SM (29,30). The physical origin of this interaction can be explained by an umbrella model (31). In this model, cholesterol must rely on the headgroup of SM to cover its large nonpolar cross section from the water. A reduction of the headgroup size of SM by removal of the three choline methyl groups leads to a molecule that fails to form liquid-ordered domains with cholesterol (32). In contrast, the interaction with cholesterol is less dependent on the chain length of the sphingomyelins (18). It has been shown that in lamellar liquid crystalline bilayers the rigid ring system of cholesterol is localized around the C9 position of the neighboring phospholipid in the membrane (33). The *cis*-double bond in the oleic acid chain at position C9-C10 renders the interaction of cholesterol with POPC less favorable. Similarly, the ability of SM with a single *cis*-unsaturation to form domains with cholesterol is strongly reduced (18).

While the formation of lateral domains in lipid membranes at low temperature has been well established, it remains open

whether (micro)domains also exist at higher, physiologically more relevant temperatures. The presence of microdomains has been described in lipid membranes (14,27,34) as well as in biological cellular membranes (35–38). On the one hand, it might be that, due to the larger thermal energy exceeding the energy of interacting lipids, those domains cannot be formed. On the other hand, domains may exist at higher temperatures in the form of very small inhomogeneities which cannot be detected due to their small size, e.g., by fluorescence microscopy. The search for domains in lipid membranes at larger temperature also points to the question for the presence of domains in intact biological membranes, which has not been answered so far. Cellular membranes are more complex systems and there are a lot of limiting factors causing smaller and nondetectable dimensions of domains than those reported in model membranes (39). Very recently, a phase separation of proteins and lipids was found in giant plasma membrane vesicles, which has been derived from cells by chemically induced or solvent-induced vesiculation (40). The size of these domains was in the micrometer-scale, as visualized by fluorescence microscopy.

In this article the lateral organization of binary and ternary mixtures of model membranes composed of PSM, POPC, and cholesterol at a molar mixing ratio of 37.5:37.5:25 was investigated by solid-state ^{2}H NMR and electron paramagnetic resonance (EPR) spectroscopy as well as confocal fluorescence microscopy. Three issues were particularly addressed in the study:

1. How does the distribution of cholesterol in the ternary mixture change upon decreasing temperature and formation of large domains?
2. What are the properties of each lipid in the ternary mixture?
3. How are the lipids laterally organized at a temperature where no domains/rafts can be detected by fluorescence microscopy?

EXPERIMENTAL PROCEDURES

Chemicals

The lipids 1-palmitoyl-2-oleoyl-*sn*-glycero-3-phosphocholine (POPC), 1-palmitoyl-d_{31}-2-oleoyl-*sn*-glycero-3-phosphocholine (POPC-d_{31}), *N*-palmitoyl-*D-erythro*-sphingosylphosphorylcholine (PSM), *N*-palmitoyl-d_{31}-*D-erythro*-sphingosylphosphorylcholine (PSM-d_{31}), 1-palmitoyl-2-[6-[(7-nitrobenz-2-oxa-1,3-diazol-4-yl)amino]caproyl]phosphatidylcholine (NBD-PC), and cholesterol were purchased from Avanti Polar Lipids (Alabaster, AL). 25-doxyl-cholesterol (SL-Chol) was synthesized according to the protocol of Maurin et al. (41). All lipids were used without further purification.

Vesicle preparation

For ^{2}H NMR measurements, mixtures of phospholipids and sterols were prepared in chloroform/methanol mixture (1/1 v/v). The solvent was removed by rotary evaporation and the resulting lipid film was redissolved in cyclohexane and lyophilized overnight to obtain a fluffy powder. Samples were hydrated with 40 wt % deuterium-depleted H_2O and equilibrated by 10 freeze-thaw cycles and gentle centrifugation. The resulting multilamellar dispersions were transferred into 5-mm glass vials for static ^{2}H NMR experiments. The samples were stored in a –70°C freezer before NMR experiments.

For EPR measurements, lipids and SL-Chol dissolved in chloroform were combined in a glass tube and dried under a stream of nitrogen. The resulting lipid film was redissolved in cyclohexane and lyophilized over night. Lipids were resolubilized by addition of HEPES buffered saline (145 mM NaCl, 5 mM HEPES, pH 7.4) resulting in the formation of multilamellar vesicles. The final lipid concentrations were 4.9 mM lipid and 0.1 mM SL-Chol.

Preparation of giant unilamellar vesicles

Giant unilamellar vesicles (GUV) were produced from lipid films dried on indium-tin-oxide (ITO)-coated glass slides by electroswelling as originally described by Angelova et al. (42). To achieve a more homogeneous distribution of the lipids, slight modifications were made. In brief, lipid mixtures were made from stock solutions in chloroform kept at −20°C. For one preparation 100 nmol lipids (including cholesterol) were used. These lipids and 1 nmol of NBD-PC were mixed to 30 μl of chloroform. After evaporation of chloroform under a nitrogen stream, lipids were dissolved in 30 μl trifluoroethanol. Single drops of the lipid mixture were pipetted onto two ITO slides (15 μl each) and allowed to spread. To obtain homogenously distributed lipid films, the solvent was evaporated on a heater plate at 50–60°C. To remove traces of the solvent, the glass slides were stored in vacuum (<10 mbar) for 1 h. The electroswelling chamber was assembled from both lipid ITO-coated slides using 1 mm Teflon spacers. The chamber was filled with 1 ml of prewarmed (50–60°C) sucrose-buffer (250 mM sucrose; 15 mM NaN_3) with an osmolarity of 280 mOsm. Immediately an alternating voltage (rising from 20 mV to 1.1 V over 30 min) with a frequency of 10 Hz was applied. GUV formed during 2 h incubation at 50–60°C. To detach the vesicles, a voltage of 1.3 V (4 Hz) was applied for 30 min. The vesicles were stored in the dark at ambient temperature for up to four days until use.

NMR measurements

^{2}H NMR spectra were recorded on a wide-bore Avance 750 NMR spectrometer (Bruker BioSpin, Rheinstetten, Germany) at a resonance frequency of 115.1 MHz (magnetic field strength of 17.6 T) for ^{2}H using a single-channel solids probe with a 5 mm solenoid coil. The ^{2}H NMR spectra were accumulated using the quadrupolar echo sequence (43) and a relaxation delay of 2 s. The two 2.5 μs $\pi/2$ pulses were separated by a 60-μs delay. Typically, 512 scans with a spectral width of 500 kHz were acquired. For all experiments, the carrier frequency of the spectrometer was placed in the center of the spectrum. The free induction decays were left-shifted after acquisition to initiate Fourier transformation on top of the quadrupolar echo. Only data from the real channel were processed to yield symmetrized ^{2}H spectra with a better signal/noise ratio.

^{2}H NMR spectra were dePaked (44), and smoothed order parameters (45) for each methylene group in the chain were determined from the observed quadrupolar splittings $\Delta\nu_Q^{(i)}$ for the i^{th} chain segment according to

$$\left|\Delta\nu_Q^{(i)}\right| = \frac{3}{4}\chi_Q\left|S_{CD}^{(i)}\right|. \quad (1)$$

Here $\chi_Q = e^2qQ/h$ represents the quadrupolar coupling constant (167 kHz for the C-^{2}H bond), $S_{CD}^i = \frac{1}{2}\langle 3\cos^2\theta_i - 1\rangle$ is the segmental order parameter, θ is the angle between the bilayer director, and the external magnetic field B_0.

The Pake doublets were assigned starting from the terminal methyl group exhibiting the smallest quadrupolar splitting. The methylene groups were assigned successively according to their increasing quadrupolar splittings. The smoothed order parameter profiles were determined from the observed quadrupolar splittings as described in detail in Huster et al. (27). Average

order parameters were calculated by adding all chain order parameters and dividing them by the number of methylene and methyl groups in the chain.

The chain extension L_C^* can be estimated by projection of the averaged length of the carbon segments on the bilayer normal and summation over successional carbon segments (46). The first moment of the deuterium spectra was calculated according to

$$M_1 = \int_0^\infty \omega f(\omega) d\omega \Big/ \int_0^\infty f(\omega) d\omega, \quad (2)$$

where $f(\omega)$ is the spectral intensity distribution and $\omega = 0$ corresponds to the Larmor frequency ω_0.

Fluorescence microscopy

To study the lateral distribution of phospholipids, 75 μl of the GUV solution were mixed with 225 μl of buffer (280 mM glucose, 11.6 mM potassium phosphate, pH 7.2, osmolarity 300 mOsm). For microscopy, the sample was placed in a drop on a coverslip. GUVs were allowed to settle on the bottom due to their greater specific density. Before imaging, the sample was incubated for 7 min at the desired temperature adjusted by a heated microscopy stage.

Images of the equatorial plane of the GUV were taken by confocal laser scanning microscopy. All images were taken with an inverted IX81 fluorescence microscope equipped with a Fluoview 1000 scanhead and a 60× (N.A. 1.35) oil-immersion objective from Olympus (Hamburg, Germany) at the respective temperature. The green NBD-fluorescence was excited with the 488 nm laser line of an Ar-ion laser. The emission of NBD was recorded in the range between 500 nm and 530 nm.

EPR measurements

EPR spectra of multilamellar vesicles were recorded at different temperatures on a X-band spectrometer EMX (Bruker, Karlsruhe, Germany) with the following parameters: modulation amplitude 1 G, power 20 mW, scan width 100 G, accumulation nine times. From the spectra of SL-Chol, the width of the midfield peak (ΔH_0) and the outer hyperfine splitting were estimated.

RESULTS AND DISCUSSION

Phase behavior of palmitoyl-sphingomyelin

First, we measured the temperature dependence of ^{2}H NMR spectra of multilamellar vesicles composed solely of PSM-d_{31} with a deuterated palmitoyl chain. The ^{2}H NMR spectra are shown in Fig. 2. At lower temperatures, the broad powder pattern is indicative of a characteristic gel phase spectrum without fine structure, except for the terminal methyl groups. By heating up the sample, well-resolved quadrupolar splittings characteristic for the liquid crystalline phase state of the lipids appear above the main transition temperature at 311 K in good agreement with literature (47). The exact phase transition temperature can be determined by analyzing the temperature dependence of the first spectral moment M_1 that reflects changes of the order of the acyl chains. Given the fact that the first spectral moment is proportional to the averaged order parameter, M_1 is a convenient tool to study changes in molecular order induced by temperature variation in the liquid crystalline phase state (48). Fig. 3 shows a dramatic decrease of the first spectral moment at 311 K associated with the main phase transition of PSM. This value is 3 K lower than found in literature (49) but a small decrease of the phase transition temperature is a known feature of deuterated lipids. When the temperature is raised above the main transition temperature, well-resolved ^{2}H NMR spectra composed of a superimposition of Pake doublets are detected. The maximal quadrupolar splitting is 34 kHz. Above the main transition temperature, the reduction of M_1 (i.e., molecular order parameter with increasing temperature) can be attributed mainly to a change in order of the first two-thirds of the chain, starting at the carbonyl group with the related reduction of chain length (50).

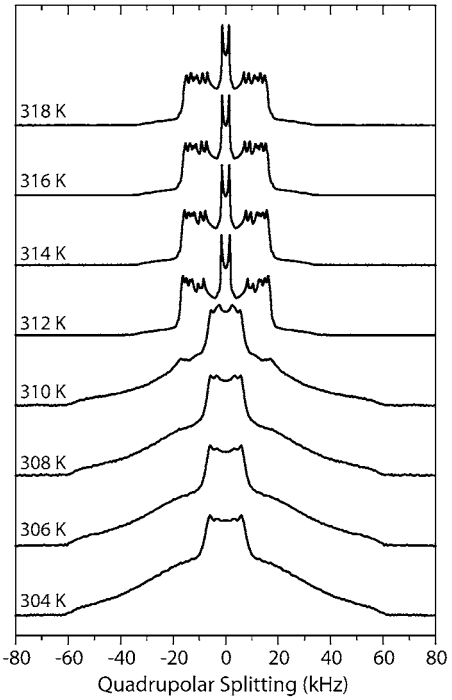

FIGURE 2 Selected ^{2}H NMR spectra of PSM-d_{31} multilamellar vesicles at 40 wt % water content as a function of temperature between 304 and 318 K. Spectra were recorded at a resonance frequency of 115.1 MHz.

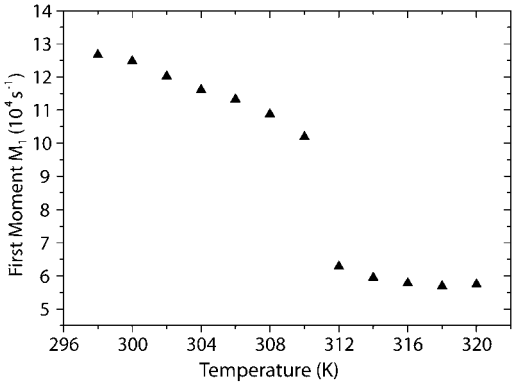

FIGURE 3 First moment M_1 of the ^{2}H NMR spectra of PSM-d_{31} multilamellar vesicles with a water content of 40 wt % as a function of temperature. As the temperature increases, the first spectral moment shows a dramatic decrease at 311 K, the main phase transition of the lipid.

Temperature-induced variations of the lipid distribution in the ternary mixture

The next goal of this study was to investigate the ternary mixture of PSM/POPC/cholesterol 37.5:37.5:25 (mol/mol/mol) with special regard to the lateral lipid organization as well as the cholesterol distribution in the liquid crystalline phase state. According to the literature, this mixture falls into the l_o/l_d coexistence region in the phase diagram at 310 K (51). To optically characterize the domain structure of the lipid mixture and to determine the temperature, at which the heterogeneous lipid distribution is abolished, we carried out confocal fluorescence microscopy experiments on GUV, which contained 1 mol % of fluorescent NBD-PC. NBD-PC is known to accumulate in the liquid-disordered l_d phase (52). A set of GUV images at varying temperatures is shown in Fig. 4. At temperatures $\leq$308 K, the pattern of NBD-PC fluorescence reflects the typical domain structure observed in these mixtures. The dark areas in the images refer to NBD-PC depleted l_o domains. Self-quenching of the NBD-lipids as an alternative explanation for the dark areas can be excluded. NBD-PC, which is found only to a very small degree in the l_o phase, has a longer lifetime than in the l_d phase (unpublished data). If self-quenching was the reason for the dark lipid areas, the lifetime should become shorter, but the opposite is the case. At higher temperatures, the fluorescence is uniformly distributed all over the membrane. Technically, it is rather difficult to determine the size of the domains in the GUV at varying temperatures by fluorescence microscopy. But the images shown in Fig. 4 suggest that the domain size varies with temperature, which would reflect a redistribution of lipids in the coexistence region. To investigate the redistribution of cholesterol upon temperature changes, ^{2}H NMR and EPR experiments were conducted.

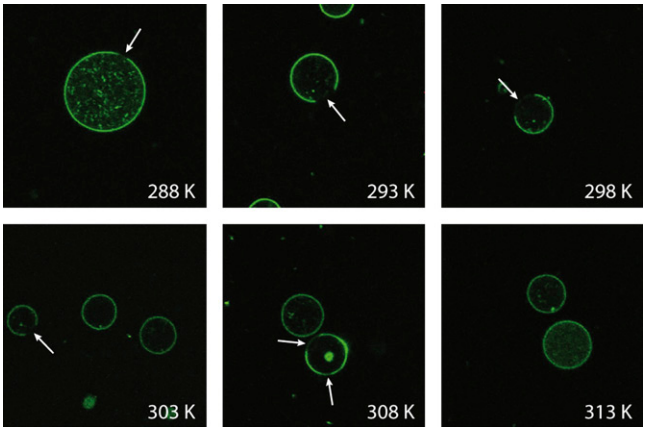

FIGURE 4 Confocal images through the equatorial plane of GUV (PSM/POPC/Chol 37.5:37.5:25) at the respective temperature. GUVs were labeled with 1 mol % of NBD-PC. Macroscopic phase separation is present at temperatures from 308 K or lower. Phase separation is indicated by the presence of dark liquid-ordered domains which are NBD-PC depleted (*arrows*).

Temperature-induced variations of the cholesterol distribution in the ternary mixture

^{2}H NMR spectroscopy is a well-suited tool to study the lipid order and chain length in the liquid crystalline phase state with great precision (48,53). However, in the gel state of a membrane or in a phase coexistence region, the ^{2}H NMR lineshapes become very difficult to interpret because of 1), the superposition of broad spectral components; 2), motionally averaged spectra; and 3), contributions from microsecond timescale motions (see Fig. 2) (14). Therefore, only a moment analysis of the spectral lineshapes provides a useful parameter. The first moments calculated from the ^{2}H NMR spectra are directly proportional to the average order parameter of the lipid chain, irrespective of the phase state of the membrane as long as the lipids undergo rapid axially symmetric reorientations. This experimental quantity can therefore be used to study lipid chain order over the phase transition, where the dePakeing procedure becomes unreliable because of limited resolution and drastic line-shape changes in the ^{2}H NMR spectra. Further, the ^{2}H NMR approach has the advantage that either the PSM or the POPC can be observed by selective deuteration of the palmitoyl chain of the respective lipids. Switching this ^{2}H label between palmitoyl chain perdeuterated PSM and POPC in the sample conveniently allows determining the properties of each phospholipid in the mixture in an unperturbed fashion. Therefore, the temperature-induced order changes of either phospholipid species in the mixture can be investigated separately by this technique.

The plots of the first spectral moments of ternary POPC/PSM/Chol mixtures (37.5:37.5:25 mol/mol/mol) are shown for PSM-d_{31} (Fig. 5 *A*) and for POPC-d_{31} (Fig. 5 *B*). Upon cooling of the sample, the first spectral moments of the ^{2}H NMR spectra increase more or less linearly, which is a trivial temperature effect since molecular order increases upon temperature decrease. However, there is a significant difference in the slope of the curves between PSM and POPC in the ternary mixture, which suggests that changes in the first spectral moments of the individual phospholipids in the mixture may, in addition to temperature, be related to changes in the cholesterol distribution between the two phospholipid species. It is well known that cholesterol produces a highly specific condensation of phospholipids, i.e., an increase in the chain order of the membrane (24,25).

To separate the temperature effect from the cholesterol-induced condensation of the phospholipids, we also studied binary phospholipid/cholesterol (37.5:25 mol/mol) mixtures. As shown in Fig. 5 *A*, the first moments of PSM-d_{31} in the presence of cholesterol increase upon decreasing temperature showing a characteristic slope. In the ternary mixture, decreasing temperature also leads to an increase in first spectral moment for PSM-d_{31}; however, the slope is approximately a factor of $\sim$2.4 steeper compared with the binary mixture. This means that the increase of the order parameter of PSM in

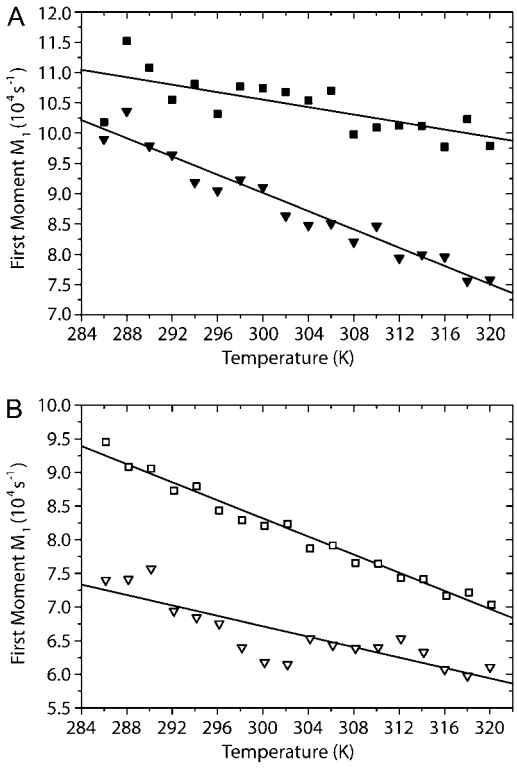

FIGURE 5 First spectral moments M_1 of ^{2}H NMR spectra of multilamellar vesicles composed of (*A*) PSM-d_{31}/Chol 37.5:25 (mol/mol) (■); PSM-d_{31}/POPC/Chol 37.5:37.5:25 (mol/mol/mol) (▼); (*B*) POPC-d_{31}/Chol 37.5:25 (mol/mol) (□); and POPC-d_{31}/PSM/Chol 37.5:37.5:25 (mol/mol/mol) (∇) as a function of temperature.

the ternary mixture is caused by the temperature decrease and by an additional effect. The latter one could be explained by a redistribution of cholesterol into the large l_o PSM/cholesterol domains that are formed at lower temperature. Since cholesterol condenses saturated chains, the more strongly increasing first spectral moment of PSM in the mixture can be interpreted that the cholesterol concentration near PSM increases. In Fig. 5 *B*, the data for POPC-d_{31} are plotted. Again, the first moments of multilamellar vesicles composed of POPC-d_{31}/Chol (37.5:25 mol/mol) increase upon decreasing temperature. In the ternary lipid mixture, the first spectral moments of POPC-d_{31} also increase with decreasing temperature, but the slope is shallower by a factor of ~1.7. This attenuated ordering of the POPC in the ternary mixture upon decreasing temperature can be explained by a depletion of cholesterol from this lipid upon formation of the large l_o domains at lower temperatures.

These experiments suggest a temperature-dependent, more pronounced preference of cholesterol for PSM in the l_o/l_d coexistence region compared to the liquid crystalline phase state (54) leading to a redistribution of cholesterol from POPC to PSM upon cooling the mixture. By that, a largely cholesterol-depleted POPC l_d phase is formed upon lowering temperature. Therefore, the NMR experiments suggest that upon cooling and formation of larger l_o and l_d domains, the sterol is continuously depleted from the l_d phase and enriched in the l_o phase.

A previous article by Veatch et al. (14) also reported a moment analysis of DPPC/DOPC/Chol raft mixtures. Interestingly, these authors observed a plateau value in the M_1 versus T plot at the miscibility transition temperature. In our data, there is no clear indication for such a plateau. The first spectral moment decreases rather linearly with increasing temperature. In particular, this is observed for the PSM in the mixture. Veatch et al. observed the plateau for the DPPC-d_{62} in the mixture, which would be the equivalent to the PSM in the mixture used here (14). For the POPC, a vague trend for such a plateau value could be indicated in the plot, but at the current signal/noise we would not be comfortable with this interpretation. Rather, the data seem to suggest a continuous redistribution of the cholesterol in the mixture upon temperature changes.

Similar conclusions can be drawn from EPR spectra of doxyl-labeled cholesterol (SL-Chol) recorded in different mixtures of PSM, POPC, and cholesterol. SL-Chol has been shown to be a good analog for native cholesterol (55). A summary of the parameters determined from ESR spectra of binary and ternary lipid mixtures at different temperatures is given in Fig. 6. Upon lowering the temperature, we observed for SL-Chol an increase of the linewidth of the midfield peak (ΔH_0) and of the outer hyperfine splitting for the raft mixture as well as for the binary POPC/Chol and PSM/Chol mixtures. These parameters reflect the amplitude of cholesterol motions in the mixture, indicating smaller motional amplitudes (i.e., higher order parameters) at lower temperatures as expected. In the liquid crystalline phase state, ΔH_0 and the outer hyperfine splitting are relatively similar in the ternary and binary mixtures, indicating that the properties of the different membranes become more similar as the lipids mix more homogeneously.

Both ^{2}H NMR moment analysis of POPC and PSM and the EPR spectroscopic characterization of SL-cholesterol in ternary raft mixtures show that cholesterol redistributes (laterally) in the plane of the membrane upon cooling. The concentration of cholesterol near PSM is increased while POPC is gradually depleted of cholesterol. The changes in the cholesterol distribution are gradual with temperature leading to a nonabrupt reorganization of the lateral arrangement within the membrane. This supports a dynamic view of lipid domains, which are also known for biological rafts (56).

Characterization of ternary mixtures of POPC/PSM/cholesterol at 313 K

The fluorescence microscopy experiments suggest that the three lipids of the raft mixture are homogeneously distributed at a temperature above ~310 K because no large domains are detected at the optical length scale. At a specific temperature, the domains appear abruptly. However, this method is not

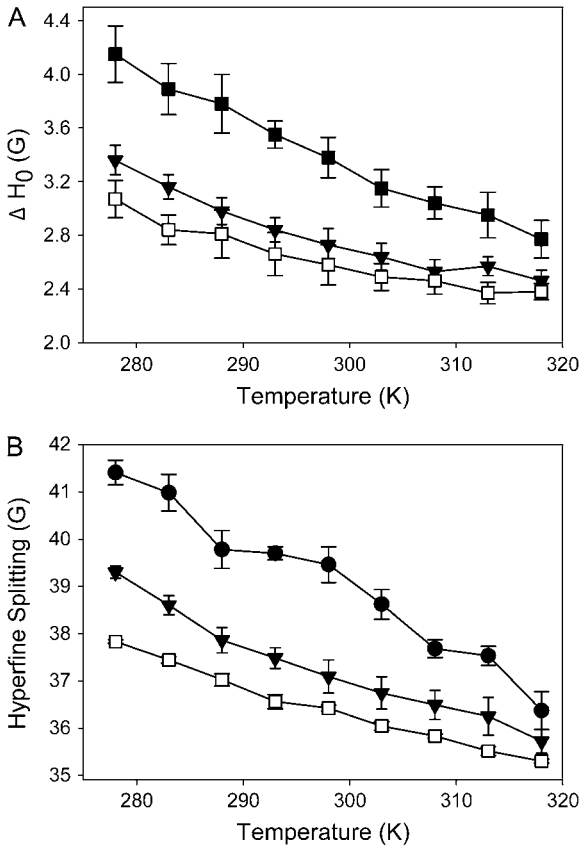

FIGURE 6 EPR parameters of SL-Chol in multilamellar vesicles consisting of PSM/POPC/Chol 37.5:37.5:25 (mol/mol/mol) (▼); POPC/Chol 37.5/25 (mol/mol) (□); and PSM/Chol 37.5:25 (mol/mol) (■,●). EPR spectra were recorded at varying temperature as described in Materials and Methods. From the spectra were estimated the line width of the midfield peak (*A*) and the outer hyperfine splitting (*B*). The data are shown as mean ± standard error.

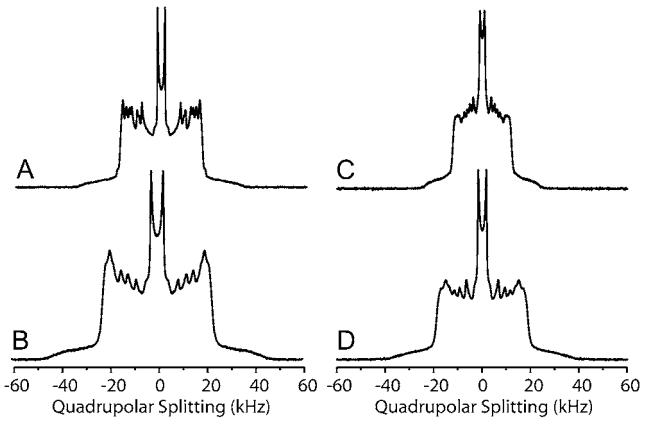

FIGURE 7 ^{2}H NMR spectra of multilamellar vesicles composed of (*A*) PSM-d_{31}, (*B*) PSM-d_{31}/POPC/Chol 37.5:37.5:25 (mol/mol/mol), (*C*) POPC-d_{31}, and (*D*) POPC-d_{31}/PSM/Chol 37.5:37.5:25 (mol/mol/mol) at a water content of 40 wt % and a temperature of 313 K. Spectra were recorded at a resonance frequency of 115.1 MHz.

sensitive to lateral heterogeneities of the submicrometer length scale. Nevertheless, biological raft structures may have significantly smaller sizes (35–38) and there are also indications that inhomogeneous lipid distributions of much smaller size exist in the liquid crystalline phase state (27). To study the properties of the mixed membrane in the liquid crystalline phase state in more detail, the temperature of 313 K was chosen.

The packing properties of the lipid molecules in ternary POPC/PSM/cholesterol mixtures at 313 K were studied by solid-state ^{2}H NMR spectroscopy using the palmitoyl chain deuterated phospholipids again. Typical ^{2}H NMR spectra of membranes of the ternary mixtures and of the isolated phospholipids at 313 K are shown in Fig. 7. One can easily see that the ^{2}H NMR spectra of PSM are significantly broader than those of POPC both in the ternary mixture and for the isolated lipid. To quantitatively discuss these differences, order parameter profiles were calculated and are shown in Fig. 8. As indicated by the shape of the ^{2}H NMR spectra, the order parameters of PSM are higher than those of POPC throughout the chain both for isolated phospholipids and the mixture. To compare numbers, average order parameters and calculated chain extents (57) are given in Table 1. The observed changes in order parameters translate into an extension in lipid chain length, which is also reported in the table.

It is a trivial fact that the order parameters of different phospholipid species in mixed membranes can be quite different, but in an ideally homogeneously mixed membrane these differences should vanish (27,58). For isolated PSM and POPC, the difference in average order parameters is 0.077 while in the PSM/POPC/Chol mixture this difference decreases to 0.066 (Table 1). This is a significant discrepancy, which results in a difference in chain extent of 1.34 Å between the two phospholipids chains, suggesting that the

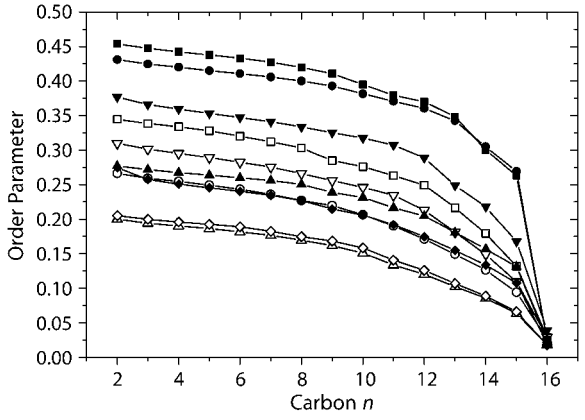

FIGURE 8 Smoothed order parameter profiles calculated from the ^{2}H NMR spectra of multilamellar vesicles composed of PSM-d_{31} (▲), PSM-d_{31}/Chol 37.5:12.5 (mol/mol) (●), PSM-d_{31}/Chol 37.5:25 (mol/mol) (■), PSM-d_{31}/POPC (mol/mol) (♦), and PSM-d_{31}/POPC/Chol 37.5:37.5:25 (mol/mol/mol) (▼); and POPC-d_{31} (△), POPC-d_{31}/Chol 37.5:12.5 (mol/mol) (○), POPC-d_{31}/Chol 37.5:25 (mol/mol) (□), POPC-d_{31}/PSM (mol/mol) (◇), and POPC-d_{31}/PSM/Chol 37.5:37.5:25 (mol/mol/mol) (∇) at 313 K.

TABLE 1 Order parameters and chain lengths (46) determined from ^{2}H NMR data acquired for palmitoyl-chain deuterated PSM-d_{31} and POPC-d_{31}, respectively, at 313 K and a water content of 40 wt %

	PSM-d_{31}		POPC-d_{31}	
	$\langle S_{CD} \rangle$	Chain extent/Å	$\langle S_{CD} \rangle$	Chain extent/Å
Isolated phospholipid	0.221	13.33	0.144	11.16
Ternary mixture POPC/PSM/cholesterol 37.5:37.5:25	0.298	14.86	0.232	13.52
Phospholipids/cholesterol 37.5:12.5	0.371	16.10	0.197	12.70
Phospholipids/cholesterol 37.5:25	0.384	16.27	0.264	14.20
PSM/POPC 50:50	0.197	12.73	0.150	11.36

ternary lipid mixture may not be homogeneously mixed at 313 K.

Several scenarios should be discussed with regard to the putative nonhomogeneous mixture of these lipids.

1. The suspicion that cholesterol interaction with the two phospholipid species is not equal even in the liquid crystalline phase state is most intriguing. Such phenomena have already been observed in lipid mixtures in the liquid crystalline phase state that are not comprised of typical raft mixture components (27). To test this hypothesis, we studied binary phospholipid/cholesterol mixtures with the following rationale in mind. If the cholesterol was equally distributed between the two phospholipid species, a binary phospholipid/cholesterol mixture of a molar composition of 37.5:12.5 should provide very similar order parameters as in the ternary mixture. As seen from Fig. 8 and Table 1, this is clearly not the case. Such a PSM/cholesterol binary mixture has much higher order parameters ($S = 0.371$) than the PSM in the ternary mixture ($S = 0.298$) and the POPC/cholesterol mixture has lower order parameters ($S = 0.197$) than POPC in the ternary mixture ($S = 0.232$). Nevertheless, in a ternary as compared to a binary mixture there is an equal chance to have another SM or a POPC molecule as a nearest neighbor. The SM–SM interaction per se may result in an elevation of chain order as mentioned under Scenario 3.
2. Another theoretical option is a complete association of cholesterol with either PSM or with POPC, while the interaction of the other lipid species with cholesterol is completely absent. The scenario in which all cholesterol is associated with the POPC is a very unlikely option, as the affinity of cholesterol to egg-sphingomyelin is ~5–12-fold larger than to POPC (54). Nevertheless, we studied the order parameters of binary phospholipid/cholesterol mixtures of a molar ratio of 37.5:25 mimicking the full aggregation of either phospholipid with cholesterol in the ternary lipid mixture. The results are shown in Fig. 8 and Table 1. Both POPC and PSM in this binary mixture have much higher order parameters than in the ternary mixture. This simple-minded comparison indicates that the cholesterol in the ternary POPC/PSM/cholesterol mixture is neither equally distributed nor completely associated with either of the phospholipids.
3. Further, the mutual influence of the phospholipids also determines the order parameters and the cross-sectional area in the mixture. The isolated phospholipids have very different order parameters in membranes (see Table 1; 0.221 for PSM and 0.144 for POPC). These differences are largely retained in a binary mixture of the two; although only a small order parameter increase is observed for POPC (0.150 in the mixture), the order parameter decrease observed for PSM is quite significant (0.197 in the mixture). Nevertheless, the order differences are by no means negligible. The phase diagram reported by de Almeida et al. (51) indicates a nonideal miscibility of PSM and POPC. This mixture shows demixing at temperatures <303 K (47). However, at 313 K, at least no optically detectable demixing of PSM/POPC was observed. So either the different order parameters of PSM and POPC in the binary mixture report local inhomogeneities that could be termed microdomains or the observed order parameter differences are an intrinsic property of the binary PSM/POPC mixture. From the differences in the order parameters of PSM and POPC in the binary mixture, a chain length difference of 1.37 Å can be calculated (see Table 1). This is much more than the typical chain length difference between *sn*-1 and *sn*-2 chains in a phospholipid. For instance, from molecular dynamics simulations this difference is only 0.15 Å in DPPC (59) and 0.25 Å in DMPC membranes (Scott Feller, personal communication, 2007).

Regardless of a different chain length between the *sn*-1 and *sn*-2 chain of the phospholipids, these differences should not drastically affect the terminal methyl groups in the chain. Further, these groups are not influenced by any geometrical effects that might influence chain order for methylene groups of upper chain segments. For instance, in the binary mixture of PSM and POPC, the difference in the methyl quadrupolar splitting is <200 Hz, which is within the typical error margin of the ^{2}H NMR experiment and indicates a rapid exchange between the two phospholipids at these conditions. In contrast, in the ternary PSM/POPC/Chol mixture, the difference in the quadrupolar splittings of the methyl groups of the two phospholipids is 1600 Hz (Fig. 7). This means that both lipid species experience their own microenvironment, in which they have a characteristic chain length. As lateral diffusion is relatively slow, there is limited exchange of lipids between these microdomains. In case of a rapid exchange between both phospholipid species, the difference in methyl quadrupolar splitting should be close to zero. In other words, the data

suggest that both phospholipids sense a different environment in the ternary mixture. So we can conclude that relatively small inhomogeneities and microdomains exist in the liquid crystalline phase state even at 313 K. The size of these heterogeneities can be estimated from the lifetime of one lipid species in its respective microdomain, which is $\sim\tau = (2\pi\Delta\nu)^{-1} = 1 \times 10^{-4}$ s. From the lipid diffusion constant (D) in the presence ($\sim 5 \times 10^{-12}$ m^2/s) and in the absence of cholesterol ($\sim 12 \times 10^{-12}$ m^2/s) (60), the minimal radius of the microdomains ($r \geq 2\sqrt{D\tau}$) would be between ~45 and 70 nm.

This number is considered an estimate and no information about the populations of each lipid in the different microenvironment can be given, because no resolved quadrupolar splittings for each microenvironment is detected at this high temperature. The fact that we see only one methyl splitting when using PSM-d_{31} indicates that these molecules are experiencing an averaged environment. The fact that we see a single but different methyl splitting when using POPC-d_{31} indicates that those molecules are experiencing a differently averaged environment. We interpret this as an argument for heterogeneity.

It should be noted that ^{2}H order parameters alone may not provide conclusive insights into the lateral organization of complex lipid mixtures. However, from the physicochemical point of view, in an ideally mixed bilayer consisting of lipid species A and B, the interaction energies between A-A and B-B should be identical to that between A and B. Since order parameters report the average lipid chain length, differences in order parameters in an ideal mixture report differences in the acyl-chain lengths of these lipids. This means that hydrophobic segments would be exposed to water or would have to interdigitate. Such effects must lead to interaction energies between the unlike lipids that are different from those of the like lipids, which may lead to lateral segregation. Of course, also mixing entropy effects contribute to the Gibbs free energy, which could mean that very small order parameter differences could be tolerated in the system.

Our study on the presence of microdomains in model membranes is also important for the investigation of the lateral organization in biological membranes. Since cellular membranes are much more complex systems, domains in these membranes should have smaller and nondetectable dimensions in contrast to those reported in model membranes (39). The different biophysical properties of the l_o and l_d domains should trigger lateral separation of embedded membrane proteins and promote protein-protein interactions. Because raft domains are predominantly in the l_o phase state, proteins preferably partitioning into these domains could more readily interact and associate with each other than in the liquid-disordered state (61). Assuming a surface for a phospholipid of 70 Å^2 and for a transmembrane protein of 80 nm^2, microdomains of a radius of 45–70 nm correspond to an area, which refers to ~9000–21,000 lipid molecules or ~80–190 protein molecules. We note that these values represent a lower limit and the actual sizes of microdomains might be larger yet below the detection limit of light microscopy.

Most likely driving the formation of these microdomains are the different interaction energies between the lipid molecules (10). The exact values for the energies of lipid-lipid interactions are not known, but have recently been estimated for a lattice model for SM/POPC/Chol (62). While the lipid-lipid interaction Gibbs energies between SM and Chol are attractive, the interaction between POPC/Chol and SM/POPC are weakly repulsive. This triggers the formation of high temperature microdomains. Domain size and morphology are a function of temperature as the interaction energy between lipid species and their mixing entropy changes with temperature.

CONCLUSIONS

Taken together, the situation of the ternary mixture of POPC/PSM/Chol can be described as a heterogeneous liquid-disordered phase at temperatures above the main phase transition of the two phospholipids. The PSM and POPC exhibit rather different order parameters of their hydrocarbon chains that indicate the existence of microdomains with a minimal radius of 45–70 nm. Microdomains of such size have been described in several articles in the past (14,27,34), particularly in biological cellular membranes (35–38). Such domain sizes are indistinguishable from uniform mixtures by fluorescence microscopy. Upon temperature decrease, we have observed a tendency for a redistribution of the cholesterol such that the l_d POPC phase is increasingly depleted of cholesterol and the l_o phase of PSM will become enriched in the sterol. However, the ^{2}H NMR data do not support a complete redistribution of the cholesterol into either of the two phases.

This study was supported by grants from the German Research Council (DFG HU 720/5-2 and Mu 1017/5-1, and GRK 1026 ''Conformational Transitions in Macromolecular Interactions'').

REFERENCES

1. Singer, S. J., and G. L. Nicolson. 1972. Fluid mosaic model of structure of cell membranes. *Science*. 175:720–731.
2. Lee, A. G. 1977. Lipid phase transitions and phase diagrams. 2. Mixtures involving lipids. *Biochim. Biophys. Acta.* 472:285–344.
3. Mabrey, S., and J. M. Sturtevant. 1976. Investigation of phase transition of lipids and lipid mixtures by high sensitivity differential scanning calorimetry. *Proc. Natl. Acad. Sci. USA*. 73:3862–3866.
4. Simons, K., and E. Ikonen. 1997. Functional rafts in cell membranes. *Nature*. 387:569–572.
5. Smart, E. J., G. A. Graf, M. A. McNiven, W. C. Sessa, J. A. Engelman, P. E. Scherer, T. Okamoto, and M. P. Lisanti. 1999. Caveolins, liquid-ordered domains, and signal transduction. *Mol. Cell. Biol.* 19:7289–7304.
6. Simons, K., and D. Toomre. 2000. Lipid rafts and signal transduction. *Nat. Rev. Mol. Cell Biol.* 1:31–39.
7. Anderson, R. G. W., and K. Jacobson. 2002. Cell biology—a role for lipid shells in targeting proteins to caveolae, rafts, and other lipid domains. *Science*. 296:1821–1825.

8. Munro, S. 2003. Lipid rafts: elusive or illusive? *Cell.* 115:377–388.
9. Binder, W. H., V. Barragan, and F. M. Menger. 2003. Domains and rafts in lipid membranes. *Angew. Chem. Int. Ed. Engl.* 42:5802–5827.
10. Almeida, P. F. F., A. Pokorny, and A. Hinderliter. 2005. Thermodynamics of membrane domains. *Biochim. Biophys. Acta.* 1720:1–13.
11. Feigenson, G. W., and J. T. Buboltz. 2001. Ternary phase diagram of dipalmitoyl-PC/dilauroyl-PC/cholesterol: nanoscopic domain formation driven by cholesterol. *Biophys. J.* 80:2775–2788.
12. Stottrup, B. L., D. S. Stevens, and S. L. Keller. 2005. Miscibility of ternary mixtures of phospholipids and cholesterol in monolayers, and application to bilayer systems. *Biophys. J.* 88:269–276.
13. Scherfeld, D., N. Kahya, and P. Schwille. 2003. Lipid dynamics and domain formation in model membranes composed of ternary mixtures of unsaturated and saturated phosphatidylcholines and cholesterol. *Biophys. J.* 85:3758–3768.
14. Veatch, S. L., I. V. Polozov, K. Gawrisch, and S. L. Keller. 2004. Liquid domains in vesicles investigated by NMR and fluorescence microscopy. *Biophys. J.* 86:2910–2922.
15. Wassall, S. R., M. R. Brzustowicz, S. R. Shaikh, V. Cherezov, M. Caffrey, and W. Stillwell. 2004. Order from disorder, corraling cholesterol with chaotic lipids. The role of polyunsaturated lipids in membrane raft formation. *Chem. Phys. Lipids.* 132:79–88.
16. van Duyl, B. Y., D. Ganchev, V. Chupin, B. de Kruijff, and J. A. Killian. 2003. Sphingomyelin is much more effective than saturated phosphatidylcholine in excluding unsaturated phosphatidylcholine from domains formed with cholesterol. *FEBS Lett.* 547:101–106.
17. Aussenac, F., M. Tavares, and E. J. Dufourc. 2003. Cholesterol dynamics in membranes of raft composition: a molecular point of view from ^{2}H and ^{31}P solid-state NMR. *Biochemistry.* 42:1383–1390.
18. Ramstedt, B., and J. P. Slotte. 1999. Interaction of cholesterol with sphingomyelins and acyl-chain-matched phosphatidylcholines: a comparative study of the effect of the chain length. *Biophys. J.* 76:908–915.
19. Ramstedt, B., and J. P. Slotte. 2006. Sphingolipids and the formation of sterol-enriched ordered membrane domains. *Biochim. Biophys. Acta.* 1758:1902–1921.
20. Kupiainen, M., E. Falck, S. Ollila, P. Niemela, A. A. Gurtovenko, M. T. Hyvonen, M. Patra, M. Karttunen, and I. Vattulainen. 2005. Free volume properties of sphingomyelin, DMPC, DPPC, and PLPC bilayers. *J. Comput. Theor. Nanosci.* 2:401–413.
21. Barenholz, Y., and T. E. Thompson. 1980. Sphingomyelins in bilayers and biological membranes. *Biochim. Biophys. Acta.* 604:129–158.
22. Marsan, M. P., I. Muller, C. Ramos, F. Rodriguez, E. J. Dufourc, J. Czaplicki, and A. Milon. 1999. Cholesterol orientation and dynamics in dimyristoylphosphatidylcholine bilayers: a solid state deuterium NMR analysis. *Biophys. J.* 76:351–359.
23. Stockton, G. W., and I. C. P. Smith. 1976. Deuterium nuclear magnetic resonance study of condensing effect of cholesterol on egg phosphatidylcholine bilayer membranes. 1. Perdeuterated fatty acid probes. *Chem. Phys. Lipids.* 17:251–263.
24. Ipsen, J. H., O. G. Mouritsen, and M. Bloom. 1990. Relationships between lipid membrane area, hydrophobic thickness, and acyl-chain orientational order. The effects of cholesterol. *Biophys. J.* 57: 405–412.
25. Oldfield, E., M. Meadows, D. Rice, and R. Jacobs. 1978. Spectroscopic studies of specifically deuterium labeled membrane systems. Nuclear magnetic resonance investigation of the effects of cholesterol in model systems. *Biochemistry.* 17:2727–2740.
26. Shaikh, S. R., V. Cherezov, M. Caffrey, W. Stillwell, and S. R. Wassall. 2003. Interaction of cholesterol with a docosahexaenoic acid-containing phosphatidylethanolamine: trigger for microdomain/raft formation? *Biochemistry.* 42:12028–12037.
27. Huster, D., K. Arnold, and K. Gawrisch. 1998. Influence of docosahexaenoic acid and cholesterol on lateral lipid organization in phospholipid mixtures. *Biochemistry.* 37:17299–17308.
28. Polozov, I. V., and K. Gawrisch. 2006. Characterization of the liquid-ordered state by proton MAS NMR. *Biophys. J.* 90:2051–2061.
29. Fielding, C. J. 2006. Lipid Rafts and Caveolae: From Membrane Biophysics to Cell Biology. Wiley-VCH, Weinheim, Germany.
30. McIntosh, T. J., S. A. Simon, D. Needham, and C. H. Huang. 1992. Structure and cohesive properties of sphingomyelin cholesterol bilayers. *Biochemistry.* 31:2012–2020.
31. Huang, J. Y., and G. W. Feigenson. 1999. A microscopic interaction model of maximum solubility of cholesterol in lipid bilayers. *Biophys. J.* 76:2142–2157.
32. Terova, B., R. Heczko, and J. P. Slotte. 2005. On the importance of the phosphocholine methyl groups for sphingomyelin/cholesterol interactions in membranes: a study with ceramide phosphoethanolamine. *Biophys. J.* 88:2661–2669.
33. Gennis, R. B. 2006. Biomembranes: Molecular Structure and Function. Springer-Verlag, New York.
34. de Almeida, R. F., L. M. Loura, A. Fedorov, and M. Prieto. 2005. Lipid rafts have different sizes depending on membrane composition: a time-resolved fluorescence resonance energy transfer study. *J. Mol. Biol.* 346:1109–1120.
35. Sharma, P., R. Varma, R. C. Sarasij, I. K. Gousset, G. Krishnamoorthy, M. Rao, and S. Mayor. 2004. Nanoscale organization of multiple GPI-anchored proteins in living cell membranes. *Cell.* 116:577–589.
36. Varma, R., and S. Mayor. 1998. GPI-anchored proteins are organized in submicron domains at the cell surface. *Nature.* 394:798–801.
37. Gaus, K., E. Gratton, E. P. Kable, A. S. Jones, I. Gelissen, L. Kritharides, and W. Jessup. 2003. Visualizing lipid structure and raft domains in living cells with two-photon microscopy. *Proc. Natl. Acad. Sci. USA.* 100:15554–15559.
38. Prior, I. A., C. Muncke, R. G. Parton, and J. F. Hancock. 2003. Direct visualization of Ras proteins in spatially distinct cell surface microdomains. *J. Cell Biol.* 160:165–170.
39. Hancock, J. F. 2006. Lipid rafts: contentious only from simplistic standpoints. *Nat. Rev. Mol. Cell Biol.* 7:456–462.
40. Baumgart, T., A. T. Hammond, P. Sengupta, S. T. Hess, D. A. Holowka, B. A. Baird, and W. W. Webb. 2007. Large-scale fluid/fluid phase separation of proteins and lipids in giant plasma membrane vesicles. *Proc. Natl. Acad. Sci. USA.* 104:3165–3170.
41. Maurin, L., P. Morin, and A. Bienvenue. 1987. A new paramagnetic analog of cholesterol as a tool for studying molecular interactions of genuine cholesterol. *Biochim. Biophys. Acta.* 900:239–248.
42. Angelova, M. I., S. Soléau, P. Méléard, J. F. Faucon, and P. Bothorel. 1992. Preparation of giant vesicles by external AC electric fields. Kinetics and applications. *Prog. Colloid Polym. Sci.* 89:127–131.
43. Davis, J. H., K. R. Jeffrey, M. Bloom, M. I. Valic, and T. P. Higgs. 1976. Quadrupolar echo deuteron magnetic resonance spectroscopy in ordered hydrocarbon chains. *Chem. Phys. Lett.* 42:390–394.
44. McCabe, M. A., and S. R. Wassall. 1995. Fast-Fourier-transform dePakeing. *J. Magn. Reson. B.* 106:80–82.
45. Lafleur, M., B. Fine, E. Sternin, P. R. Cullis, and M. Bloom. 1989. Smoothed orientational order profile of lipid bilayers by ^{2}H-nuclear magnetic resonance. *Biophys. J.* 56:1037–1041.
46. Petrache, H. I., K. C. Tu, and J. F. Nagle. 1999. Analysis of simulated NMR order parameters for lipid bilayer structure determination. *Biophys. J.* 76:2479–2487.
47. Mehnert, T., K. Jacob, R. Bittman, and K. Beyer. 2006. Structure and lipid interaction of *n*-palmitoylsphingomyelin in bilayer membranes as revealed by ^{2}H-NMR spectroscopy. *Biophys. J.* 90:939–946.
48. Davis, J. H. 1983. The Description of membrane lipid conformation, order and dynamics by ^{2}H NMR. *Biochim. Biophys. Acta.* 737: 117–171.
49. Bar, L. K., Y. Barenholz, and T. E. Thompson. 1997. Effect of sphingomyelin composition on the phase structure of phosphatidylcholine-sphingomyelin bilayers. *Biochemistry.* 36:2507–2516.
50. Holte, L. L., S. A. Peter, T. M. Sinnwell, and K. Gawrisch. 1995. ^{2}H nuclear magnetic resonance order parameter profiles suggest a change of molecular shape for phosphatidylcholines containing a polyunsaturated acyl chain. *Biophys. J.* 68:2396–2403.

51. de Almeida, R. F. M., A. Fedorov, and M. Prieto. 2003. Sphingomyelin/phosphatidylcholine/cholesterol phase diagram: boundaries and composition of lipid rafts. *Biophys. J.* 85:2406–2416.

52. Shaw, J. E., R. F. Epand, R. M. Epand, Z. G. Li, R. Bittman, and C. M. Yip. 2006. Correlated fluorescence-atomic force microscopy of membrane domains: structure of fluorescence probes determines lipid localization. *Biophys. J.* 90:2170–2178.

53. Seelig, J. 1977. Deuterium magnetic resonance—theory and application to lipid membranes. *Q. Rev. Biophys.* 10:353–418.

54. Tsamaloukas, A., H. Szadkowska, and H. Heerklotz. 2006. Thermodynamic comparison of the interactions of cholesterol with unsaturated phospholipid and sphingomyelins. *Biophys. J.* 90:4479–4487.

55. Scheidt, H. A., P. Müller, A. Herrmann, and D. Huster. 2003. The potential of fluorescent and spin-labeled steroid analogs to mimic natural cholesterol. *J. Biol. Chem.* 278:45563–45569.

56. Rietveld, A., and K. Simons. 1998. The differential miscibility of lipids as the basis for the formation of functional membrane rafts. *Biochim. Biophys. Acta.* 1376:467–479.

57. Vogel, A., C. P. Katzka, H. Waldmann, K. Arnold, M. F. Brown, and D. Huster. 2005. Lipid modifications of a Ras peptide exhibit altered packing and mobility versus host membrane as detected by ^{2}H solid-state NMR. *J. Am. Chem. Soc.* 127:12263–12272.

58. Huster, D., K. Arnold, and K. Gawrisch. 2000. Strength of Ca^{2+} binding to retinal lipid membranes: consequences for lipid organization. *Biophys. J.* 78:3011–3018.

59. Pastor, R. W., R. M. Venable, and S. E. Feller. 2002. Lipid bilayers, NMR relaxation, and computer simulations. *Acc. Chem. Res.* 35:438–446.

60. Scheidt, H. A., D. Huster, and K. Gawrisch. 2005. Diffusion of cholesterol and its precursors in lipid membranes studied by ^{1}H pulsed field gradient magic angle spinning NMR. *Biophys. J.* 89:2504–2512.

61. Samsonov, A. V., I. Mihalyov, and F. S. Cohen. 2001. Characterization of cholesterol-sphingomyelin domains and their dynamics in bilayer membranes. *Biophys. J.* 81:1486–1500.

62. Frazier, M. L., J. R. Wright, A. Pokorny, and P. F. F. Almeida. 2007. Investigation of domain formation in sphingomyelin/cholesterol/POPC mixtures by fluorescence resonance energy transfer and Monte Carlo simulations. *Biophys. J.* 92:2422–2433.